Applied Surface Science 258 (2012) 2103–2106

Contents lists available at ScienceDirect

Applied Surface Science

journal homepage: www.elsevier.com/locate/apsusc

Photocatalytic thin films containing TiO_2:N nanopowders obtained by the layer-by-layer self-assembling method

L. Rojas-Blanco [a,*], M.D. Urzúa [b], R. Ramírez-Bon [a], F.J. Espinoza Beltrán [a]

[a] Centro de Investigación y de Estudios Avanzados del Instituto Politécnico Nacional, Unidad Querétaro, Libramiento Norponiente No. 2000, Fraccionamiento Real de Juriquilla, C.P. 76230 Santiago de Querétaro, Qro., Mexico
[b] Departamento de Química, Facultad de Ciencias, Universidad de Chile, Las Palmeras 3425, Casilla 653, Santiago, Chile

ARTICLE INFO

Article history:
Available online 27 May 2011

Keywords:
Photocatalysis
Titanium oxide
Nitrogen doping
Layer by layer
Srilankite

ABSTRACT

In this work, TiO_2–N powders were synthesized by high-energy ball milling, using commercial titanium dioxide (TiO_2) in the anatase phase and urea to introduce nitrogen into TiO_2 in order to enhance their photocatalytic properties in the visible spectral region. Several samples were prepared by milling a mixture of TiO_2–urea during 2, 4, 8, 12 and 24 h and characterized by spectroscopic and analytical techniques. X-ray diffraction (XRD) results showed the coexistence of anatase and high-pressure srilankite TiO_2 crystalline phases in the samples. Scanning electron microscopy (SEM) revealed that the grain size of the powder samples decreases to 200 nm at 24 h milling time. UV–Vis diffuse reflectance spectroscopic data showed a clear red-shift in the onset of light absorption from 387 to 469 nm as consequence of nitrogen doping in the samples. The photocatalytic activity of the TiO_2–N samples was evaluated by methylene blue degradation under visible light irradiation. It was found that TiO_2–N samples had higher photocatalytic activity than undoped TiO_2 samples, which could be assigned to the effect of introducing N atoms and XPS results confirm it. Using polyethylenimine (PEI), transparent thin films of TiO_2–N nanoparticles were prepared by layer-by-layer self assembly method. UV–visible spectrophotometry was employed in a quantitative manner to monitor the adsorbed mass of TiO_2 and PEI after each dip cycle. The adsorption of both TiO_2 and PEI showed a saturation dip time of 15 min.

1. Introduction

Heterogeneous photocatalysis of organic compounds on semiconductor surfaces in aqueous media is an efficient method for waste water treatment and its use has been increased in recent years [1]. TiO_2 is a low-cost photocatalyst and is the most extensively investigated material in this field. However, its high energy band gap (3.3 eV for anatase phase) limits the photocatalytic process to irradiation wavelengths in the UV region (λ <390 nm). Such radiation corresponds to only 5% of the incident solar flux. Due to this limitation, the preparation of new photocatalysts which can be excited in the visible range is a current topic of great interest among researchers in the area. One approach is to dope with transition metals the TiO_2 lattice [2] and another one is to form coupled photocatalysts [3]. However, doped materials suffer from thermal instability and increase in carrier-recombination centers. On the other hand, coupled photocatalysts can efficiently separate photogenerated electron–hole pairs, but they are not effective in extending the wavelength range response of TiO_2 to the visible light region. One promising approach involves doping of TiO_2 with low levels of nitrogen, a process which effectively red-shifts its absorption spectrum [4–8]. Shifu et al. reported that nitrogen doping into sites of TiO_2 had proven to be indispensable for band gap narrowing and photocatalytic activity [9]. The nitrogen effective doping can be attained by various methods such as the heating of TiO_2 powder in an ammonia atmosphere over several hundred degrees [10], heating titanium hydroxide with urea [11,12] and by high energy milling of TiO_2 mixed with an organic compound such as urea as the source of nitrogen [9]. Among these methods, we are most interested in the last one because the process can provide N-doped TiO_2 in the form of nanopowders with increased high specific surface area. In addition, high energy milling is a simple processing technique which has been less explored for this purpose.

Layer-by-layer (LBL) assembly is a rich, versatile, and significantly inexpensive approach by which thin films based on sequential adsorption of oppositely charged layers by electrostatic attraction in aqueous solutions. The method provides nano-scale control on the fabrication of thin films, it is environmentally friendly, of low cost, with simple instruments which makes it ideal for practical use, and it can make uniform deposition on complex geometries. Researchers have been attracted to the fabrication of

* Corresponding author.
E-mail address: smile_liz18@hotmail.com (L. Rojas-Blanco).

0169-4332/$ – see front matter © 2011 Elsevier B.V. All rights reserved.
doi:10.1016/j.apsusc.2011.03.150

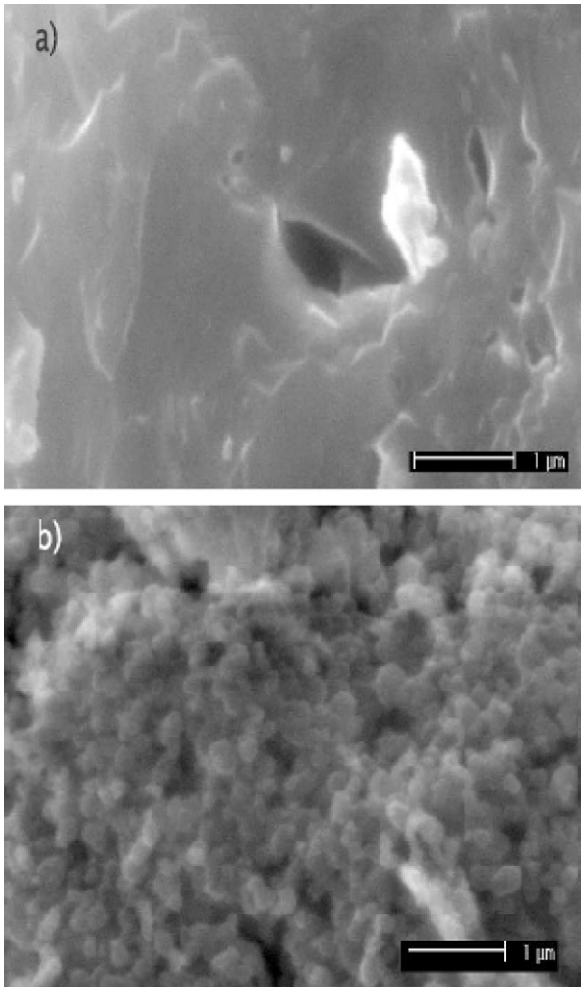

Fig. 1.

thin solid films using LBL for generating smart surfaces [13] at the molecular level for various biological and material applications.

In this paper we report the N-doping of TiO_2 obtained by high energy milling of urea and commercial TiO_2 powders. The aim of the present work is to prepare TiO_2:N powders to extend to the visible light region the photocatalytic activity of TiO_2. For this, we first studied the effect of this non-metal dopant on the crystalline structure and optical properties of TiO_2 and then evaluated its photocatalytic activity by monitoring the degradation of a model dye in solution (methylene blue) under irradiation with UV and visible light; also, we describe a method for the stepwise construction of molecular-level ordered TiO_2/polyethylenimine (PEI) nanocomposite films by a layer-by-layer self-assembly process.

2. Experimental

Nanocrystalline TiO_2:N powders were prepared by a high-energy ball mill at room temperature in a hardened steel vial with a Spex 8000 laboratory ball mill (1200 rpm) using hardened steel balls of 5.0 and 2.5 mm diameters. TiO_2 (Sigma–Aldrich 99.99% purity reactive grade) and urea (Sigma–Aldrich 99.9% purity) were milled with the molar ratio of 10:1 for 2, 4, 8, 12 and 24 h in air atmosphere. A process control agent (PCA), ethylic alcohol, was added. After milling, all the samples were annealed in air at 500 °C for 1 h.

X-ray diffraction measurement of the powder samples with different milling times was performed using Co-Kα radiation. The microstructure of TiO_2 milled particles was observed by scanning

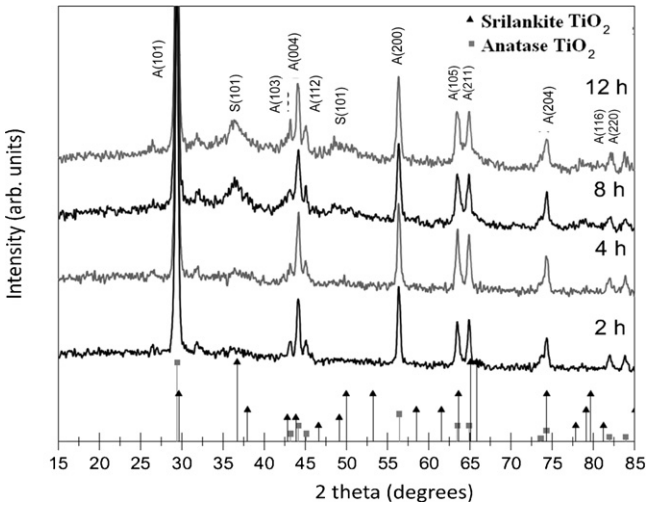

Fig. 2.

electron microscopy (SEM) with a Philips XL30SEM instrument. In the photocatalytic experiments, the TiO_2:N powders were placed into a methylene blue solution (concentration 15 mg/L), in order to study the kinetics of its degradation as a function of the exposure time to the visible light irradiation from a tungsten halogen lamp and its intensity was 100 mW/cm^2. Firstly, the powdered samples (about 200 mg) were dispersed into 200 mL 15 mg/L (Ci) of methylene blue aqueous solution stirring magnetically for 30 min to establish absorption/desorption equilibrium. Subsequently, 5 mL of the suspensions was sampled. After the suspensions were centrifuged at 2000 rpm, the concentrations (C_0) of the solutions were measured at 662 nm on a UV–vis spectrometer. At the given time intervals, 5 mL of the suspension was taken from the suspensions and their concentrations were measured. The XPS (X-ray Photoelectron Spectroscopy) data were obtained using a Thermo-Electron instrument with a XPS110 electron analyzer employing non-monocromatic Al Kα X-ray ($h\nu$ = 1486.6 eV) at 100 W with and electron take-off angle of 90°. Samples were attached on top of a sample holder by indium foil. The spectrometer is equipped with a seven-channel hemispherical detector. The lens mode used was small area XPS 600 μm with slit 0 and aperture 4. Pass energy of 100 eV for surveys and 50 eV for high resolution was used during the analysis of the samples. The scan numbers were different for each range of core level electron energy states of samples. All analyses were performed at a vacuum pressure of 3×10^{-10} Torr.

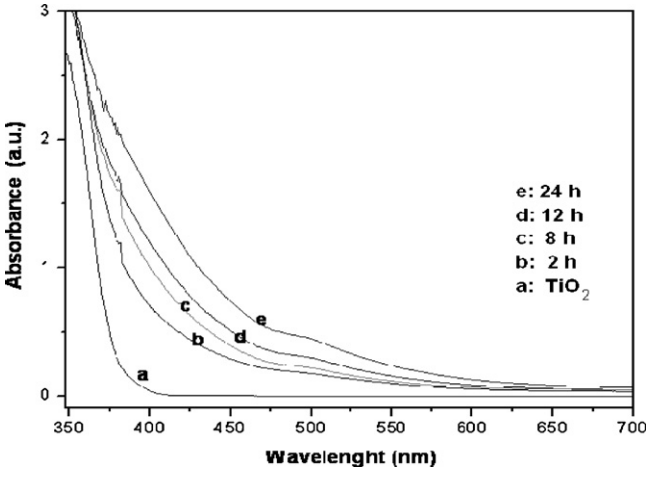

Fig. 3.

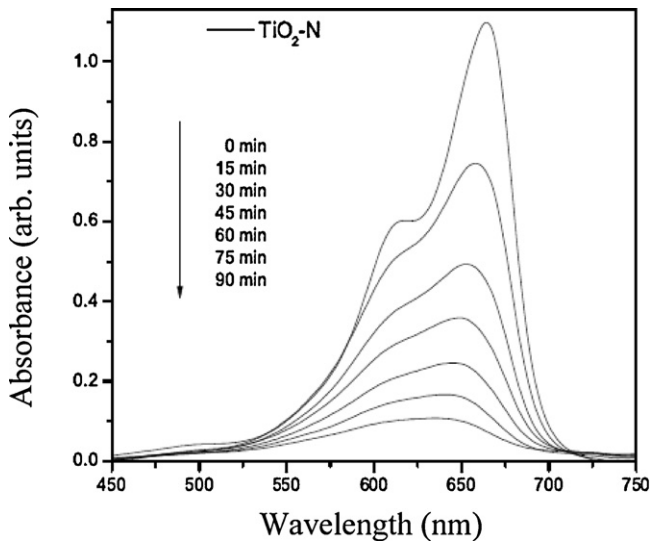

Fig. 4.

XPS measurements provided information regarding the form which nitrogen is bonding in the TiO_2 lattice. The XPS peaks were fitted into subcomponents using the software Analyzer.

For the immobilization of the TiO_2–N powders on polymer, colloidal suspension of nanoparticles was prepared by mixing powders with DI water (Milli-Q with resistance of 17.9 MΩ cm) in 1 g/L. Polyethylenimine (PEI) was purchased from Aldrich Chemical Co. and solutions of 0.1 M. pH of the solutions was set to 2–10 using HCl and NaOH (Sigma). UV–visible absorption spectra of TiO_2–N sol and PEI solutions were obtained with reference to DI water by a Lambda 950 Perkin Elmer Spectrophotometer.

Microscope glass slides were used as substrates and to give complete hydrophilicity to the substrates they were immersed for 15 min in a solution of water, ammonia and hydrogen peroxide (ratio 5:1:1, at 70 °C) and they were rinsed again in DI water and dried with nitrogen. The treated substrates were first dipped in PEI solution and rinsed in DI water and dried with mild N_2 gas stream. Film preparation continued with dipping in TiO_2–N sol with the same washing and drying procedure.

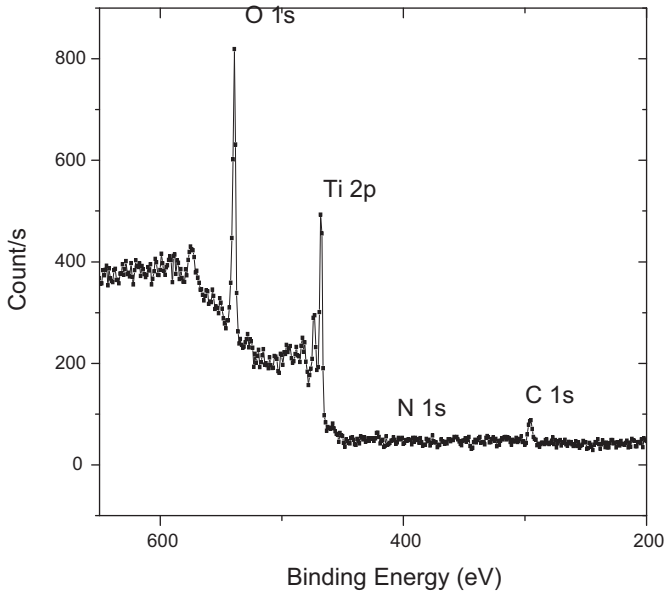

Fig. 5.

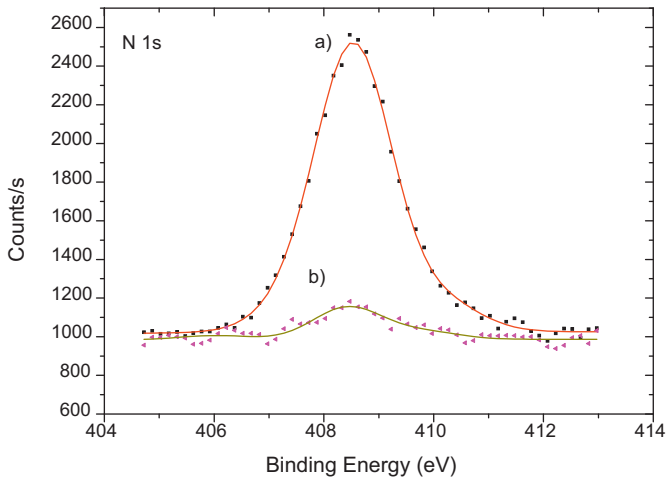

Fig. 6.

In order to find the optimum dip time for LbL, samples were prepared with up to five dip cycles ([PEI/TiO_2]5) with 15 min dip times in each solution. After each dip cycle, the UV–visible transmission spectra were obtained which were converted to absorbance ($A = -\log(T_{sample}/T_{reference})$ and $T_{reference}$ is the transmission of clean substrate in each wavelength).

3. Results and discussion

3.1. Morphological studies

Fig. 1 shows the SEM images of (a) unmilled TiO_2 sample and (b) 24 h milled TiO_2 sample. The unmilled sample shows a microstructure of irregularly shaped laminar crystals, meanwhile the milled sample shows agglomerated nanoparticles with an average size of about 200 nm.

3.2. XRD

The XRD patterns of the milled samples are shown in Fig. 2. At the bottom, the positions of the diffraction peaks of the anatase and srilankite phases of TiO_2 are indicated. The evolution of these patterns with milling time indicates that ball milling induces the crystalline phase transformation from anatase to srilankite in the

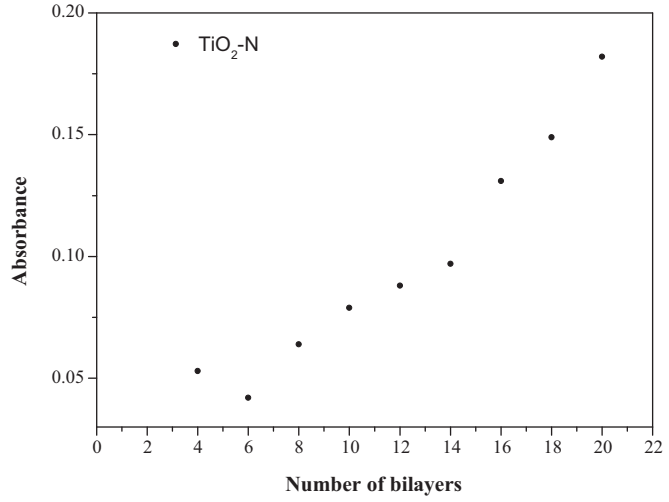

Fig. 7.

TiO_2 powders. It has been shown that the milling-induced transformations from anatase to srilankite in nanocrystalline TiO_2 are partly attributed to the rise of the local temperature and pressure at the collision sites of the powder and the balls. However, it can also be seen in this figure that not all anatase phase transforms into srilankite phase, because of the presence of anatase diffraction peaks in the milled sample patterns.

Fig. 3 shows UV–vis spectral data for the undoped and nitrogen-doped TiO_2 samples. These data reveal that nitrogen doping in TiO_2 nanoparticles shifts the absorption edge toward higher wavelength, that is, toward the visible region with a substantially long band tailing, produced by dopant-defect states. The mean band gap values are found to be 3.2 and 2.64 eV for undoped and doped samples, respectively.

The long band tail of the samples after annealing at 500 °C for 24 h shifts in the onset light absorption from 387 to 469 nm, suggesting the incorporated nitrogen. It could be ascribed to the compound effect of dopant-induced midgap electronic states and lattice disorder effects.

In order to study the effect of high-energy ball milling on the catalytic properties, the catalytic activities of the nanopowder samples were estimated by the degradation of methylene blue in solution after exposure to irradiation. Fig. 4 shows the methylene blue solution absorption spectra after different times of exposure to lamp irradiation as described in Section 2. The spectrum of the solution before light exposure displays the typical methylene blue absorption bands at about 600 and 660 nm. The decrease in the intensity of these absorption bands is due to the photodegradation of methylene blue in the presence of N-doped TiO_2 nanoparticles.

Thus, the results in Fig. 4 clearly show a significant decrease in the absorption bands intensity of methylene blue, indicating substantial degradation of the dye under the visible light dominated illumination.

3.3. XPS analysis

XPS measurements provided information about the incorporation of N into TiO_2 powder. Fig. 5 shows the XPS survey scan of the TiO_2:N sample milled for 24 h where the signals of O 1s, Ti 2p, N 1s and C 1s can be observed. High resolution XPS scans were performed to identify the chemical bonding of O, Ti and N in the milled samples. The region of O 1s peak (Fig. 6) corresponds to titanium oxide in 533.26 eV and O 1s in 532 eV. Particularity at sample with zero milled is not possible to see the titanium oxide easily, presented a suboxide of titanium in 532.29 eV. The doublet $2p_{1/2}$ (472.6 eV) and $2p_{3/2}$ (467 eV) of titanium was present in the sample. The signal of titanium $2p_{3/2}$ was presented low at zero milled. While the signal on samples with 4 and 24 h milled was present at the same position.

Fig. 6 shows the XPS results in the N 1s region for the unmilled sample and milled samples for 4 and 24 h. The N 1s peak at 402.2 eV corresponds to N in the bond N–Ti indicating that N atoms substitute O atoms in the TiO_2 lattice because in sample with 4 h the oxygen peak decreases and the nitrogen peak increases. This peak is more intense in the spectrum of the sample milled for 4 h than in the sample milled for 24 h. Taking into account that XPS is a high sensitivity surface technique this result can be an indication that N atoms lay at the surface of the samples milled for shorter times. The chemical composition was calculated for each sample using XPS intensities. Consider the cross section of each photoemission and the attenuation length to know the chemical development.

3.4. LBL immobilization

Fig. 7 displays the optical absorption of TiO_2 sol and PEI solution. One observes that the absorption peaks of TiO_2 nanoparticles and PEI chains are apart; therefore in the composite thin films of TiO_2/PEI the quantity of each part could be determined. This idea is used in this paper for the quantitative measurement of adsorbed mass of TiO_2 and PEI.

The linear nature of the plot suggests that each layer adsorbed contributes an equal amount of material to the thin film. As seen in this figure, the consecutive adsorption of layers is stepwise and the deposition process is linear and consistent from layer to layer.

4. Conclusions

In conclusion we found that N-doped titania can be prepared by a high energy ball mill using commercial titanium oxide and urea. The substitutional N doping of TiO_2 broadens the light absorption spectrum to the visible region to make it visible light active. Therefore the photocatalytic activity of TiO_2:N samples was induced by visible light as shown by the methylene blue photodegradation in our experiments. XPS measurements corroborated the incorporation of N atoms substituting O atoms in the crystalline lattice of TiO_2.

References

[1] C. Tristao, J. Magalhaes, F.P. Corio, C.M.E. Sansiviero, J. Photochem. Photobiol. 181 (2006) 152–157.
[2] K. Lee, N.H. Lee, S.H. Shin, H.G. Lee, S.J. Kim, Mater. Sci. Eng. B 129 (2006) 109–115.
[3] Y. Bessekhouad, N. Chaoui, M. Trzpit, N. Ghazzal, D. Robert, J.V. Weber, J. Photochem. Photobiol. A: Chem. 183 (2006) 218–224.
[4] R. Asahi, T. Morikawa, T. Ohwaki, K. Aoki, Y. Taga, Science 293 (2001) 269.
[5] S. Sakthivel, M. Janczarek, H. Kisch, J. Phys. Chem. B 108 (2004) 19384.
[6] S. Sakthivel, H. Kisch, ChemPhysChem 4 (2003) 487.
[7] K. Kobayakawa, Y. Murakami, Y. Sato, J. Photochem. Photobiol. A 170 (2005) 177.
[8] Z.P. Wang, W.M. Cai, X.T. Hong, X.L. Zhao, F. Xu, C.G. Cai, Appl. Catal. B 57 (2005) 223.
[9] C. Shifu, C. Lei, G. Shen, C. Gengyu, Chem. Phys. Lett. 413 (2005) 404–409.
[10] H. Irie, Y. Watanabe, K. Hashimoto, J. Phys. Chem. B 107 (2003) 5483.
[11] J. Yuan, M. Chen, J. Shi, W. Shangguan, Int. J. Hydrogen Energy 31 (2006) 1326–1331.
[12] K. Kobayakawa, Y. Murakami, Y. Sato, J. Photochem. Photobiol. A: Chem. 170 (2005) 177–179.
[13] P.T. Hammond, Adv. Mater. 16 (2004) 1271–1293.